

Supporting Information for

**Supramolecular Ternary Polymer Mediated by Cucurbituril  
and Cyclodextrin**

Qian Wang, Yong Chen and Yu Liu\*

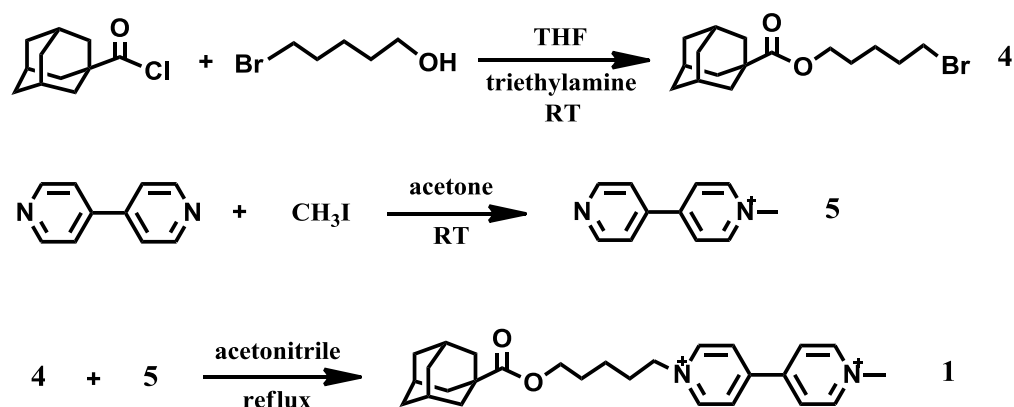
*Department of Chemistry, State Key Laboratory of Elemento-Organic Chemistry,*

*Nankai University, Tianjin, 300071, P. R. China*

*E-mail: yuliu@nankai.edu.cn Fax: (+86)22-2350-3625*

## Experimental Section

Mono-6-deoxy-6-{4-[2-hydroxyl-6-naphthylloxymethyl][1,2,3]triazolyl}- $\beta$ -CD (Np- $\beta$ -CD) was synthesized and purified referring to the literature process.<sup>1</sup>  $^1\text{H}$  NMR (400MHz,  $\text{D}_2\text{O}$ , ppm),  $\delta$  3.18-3.79 (m, 42H, H of C-3, C-5, C-6, C-2, C-4 of  $\beta$ -CD), 4.74-5.16 (m, 7H, H of C-1 of  $\beta$ -CD), 5.13-5.18 (m, 2H,  $-\text{CH}_2-$ ), 6.75-6.89 (m, 1H, H of naphthalene), 7.17 (m, 3H, H of naphthalene), 7.53-7.60 (m, 3H, H of naphthalene and triazole).



Scheme S1 Synthesis route of compound 1.

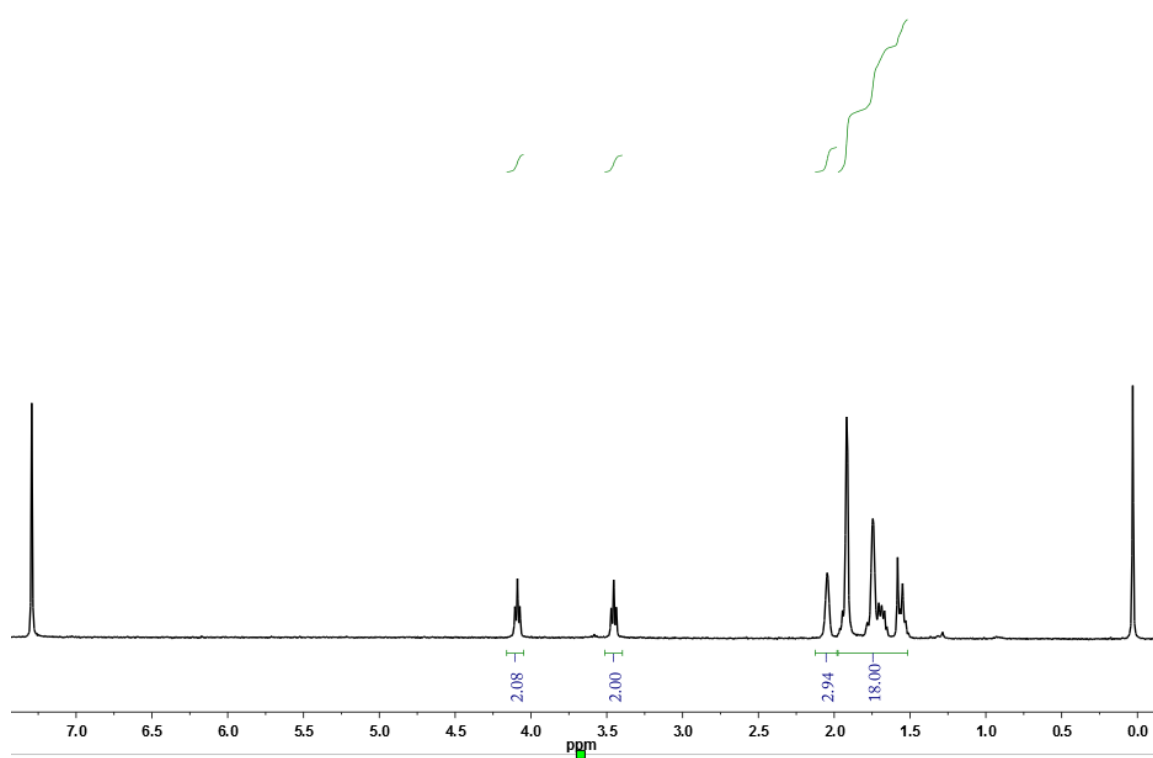


**Fig. S1.**  $^1\text{H}$  NMR spectrum (400 MHz,  $\text{D}_2\text{O}$ , 298.15K) of compound **4**.

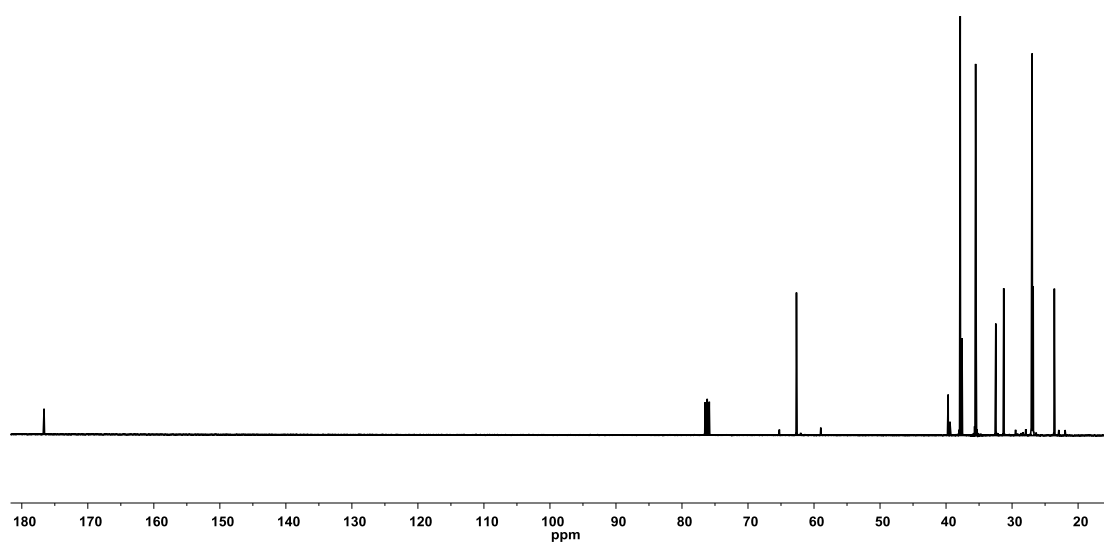


**Fig. S2.**  $^{13}\text{C}$  NMR spectrum (100 MHz,  $\text{D}_2\text{O}$ , 298.15K) of compound **4**.

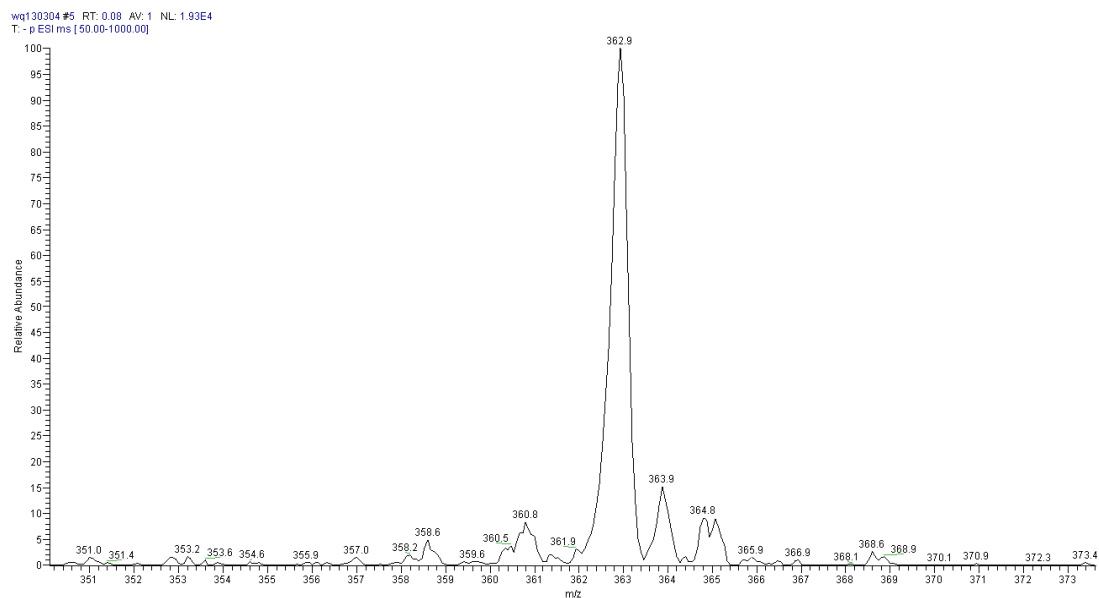


**Fig. S3.** ESI-MS spectrum of compound 4.

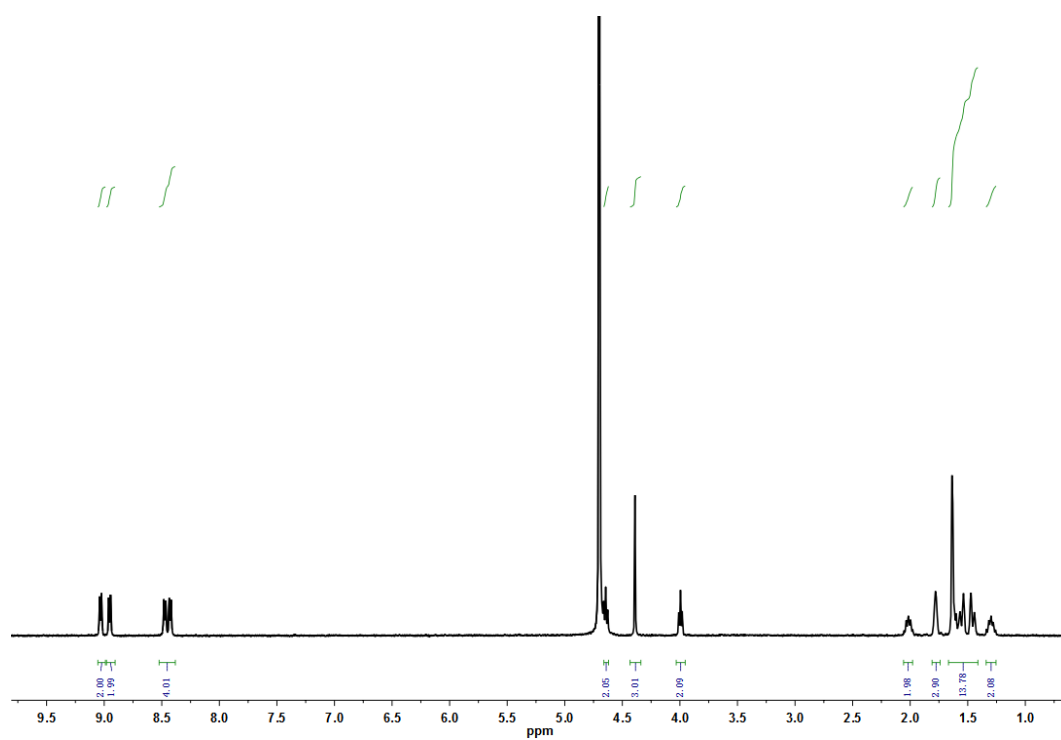


**Fig. S4.** <sup>1</sup>H NMR spectrum (400 MHz, D<sub>2</sub>O, 298.15K) of compound 1.

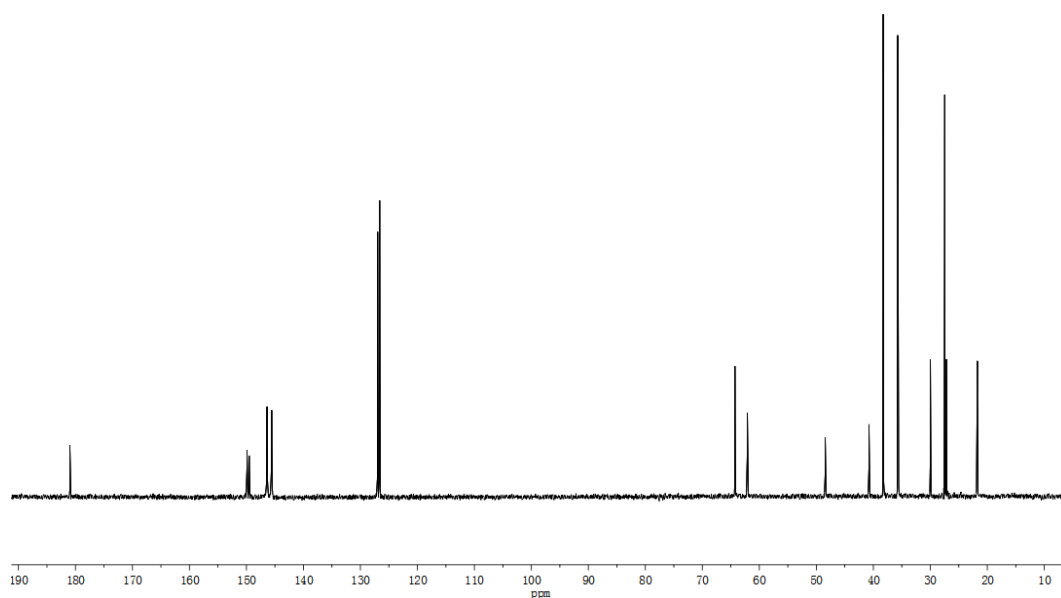


**Fig. S5.** <sup>13</sup>C NMR spectrum (100 MHz, D<sub>2</sub>O, 298.15K) of compound **1**.

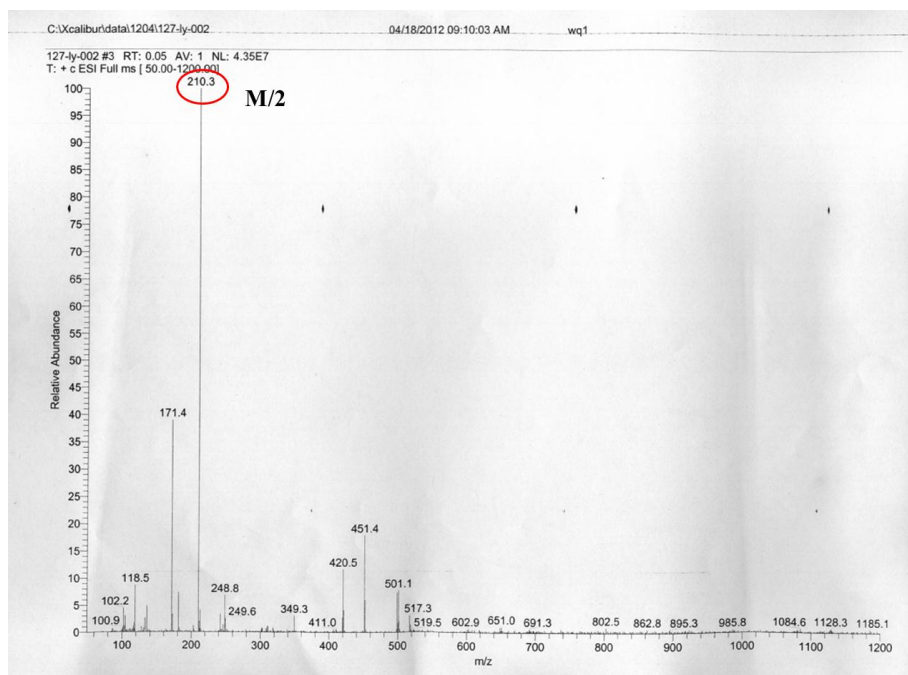


**Fig. S6.** ESI-MS spectrum of compound **1**.

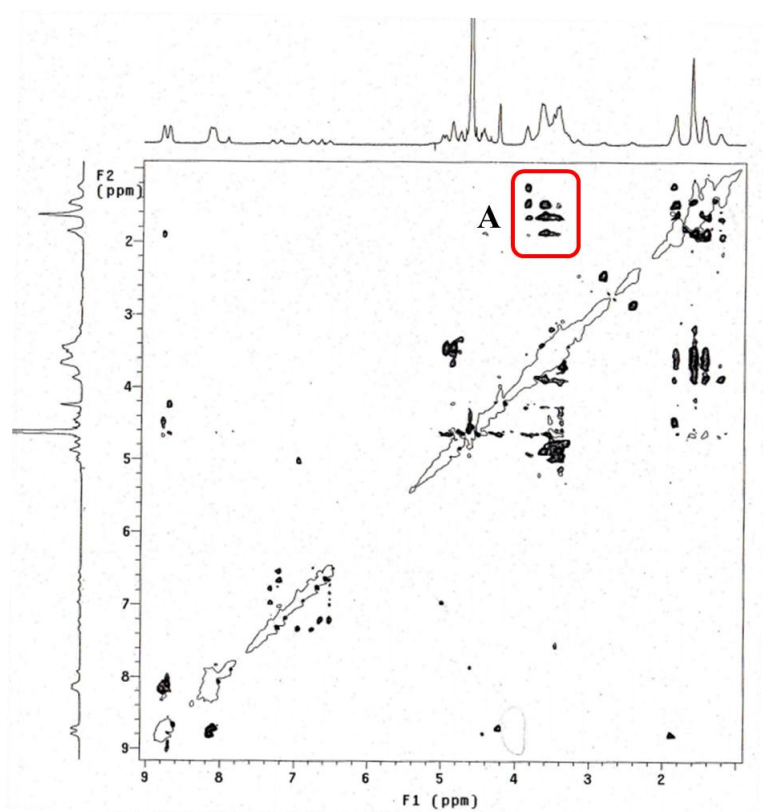


**Fig. S7.** ROESY spectrum (300 MHz) of Np- $\beta$ -CD with 1 equiv. **1** ( $1.0 \text{ mM}^{-1}$ ) in  $\text{D}_2\text{O}$  at 298.15K with a mixing time of 230 ms.

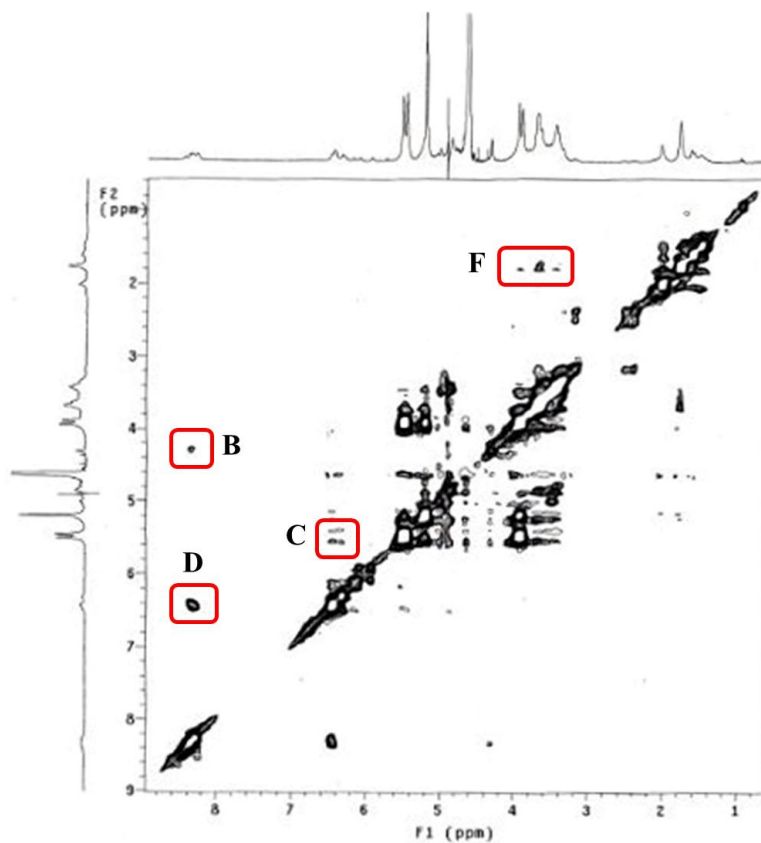


**Fig. S8.** ROESY spectrum (300 MHz) of Np- $\beta$ -CD/1 ( $1.0 \text{ mM}^{-1}$ ) with 1.0 equiv. CB[8] in  $\text{D}_2\text{O}$  at 298.15 K with a mixing time of 230 ms.

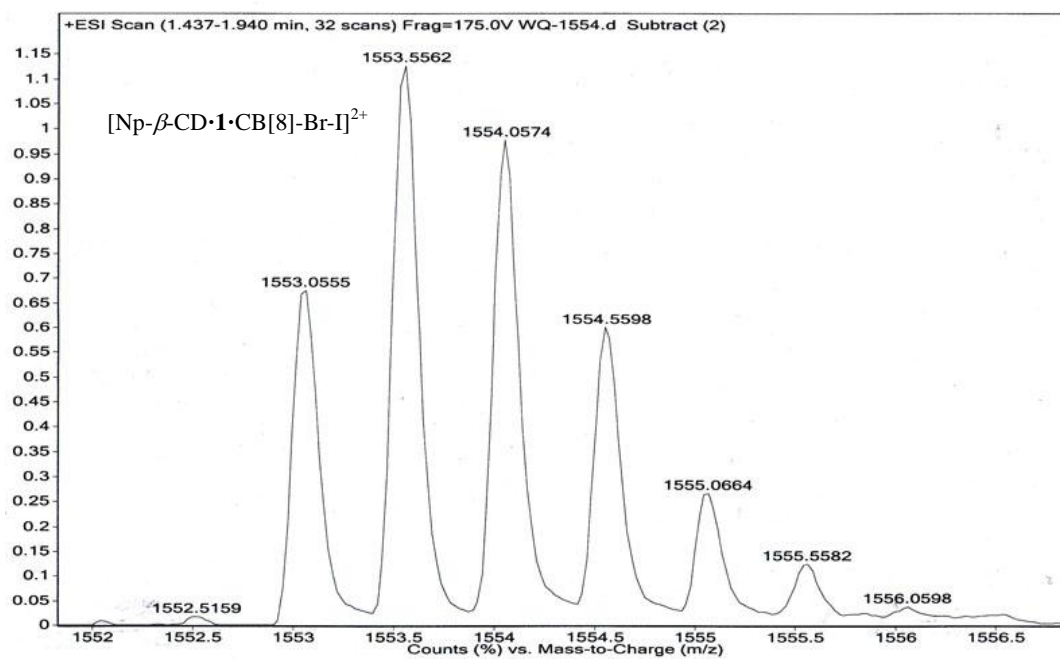


**Fig. S9.** HR-MS spectrum of ternary complex Np- $\beta$ -CD/1/CB[8].

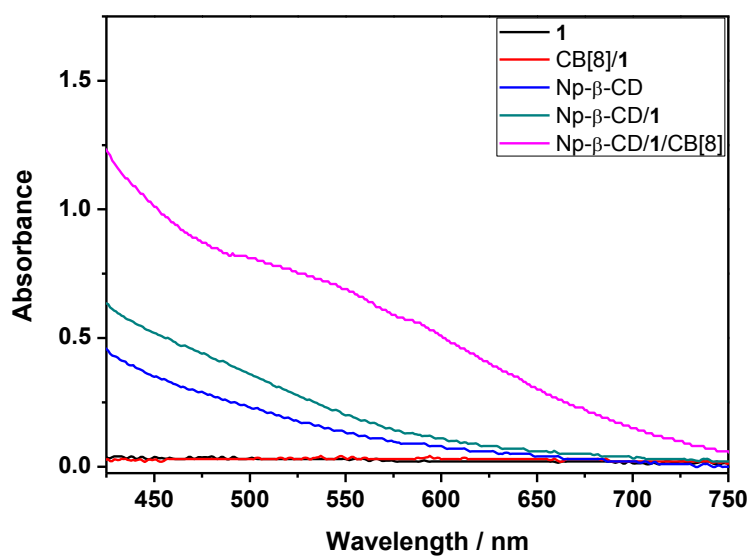


**Fig. S10.** UV spectra at 1.0 mM in H<sub>2</sub>O at 298 K.

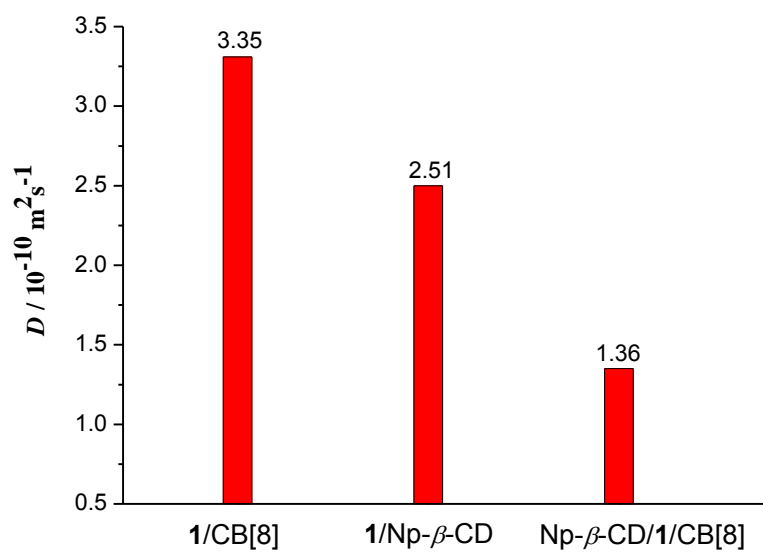


**Fig. S11.** Diffusion constants  $D$  (500MHz, D<sub>2</sub>O, 298K) of 1/CB[8], 1/Np-β-CD and Np-β-CD/1/CB[8].

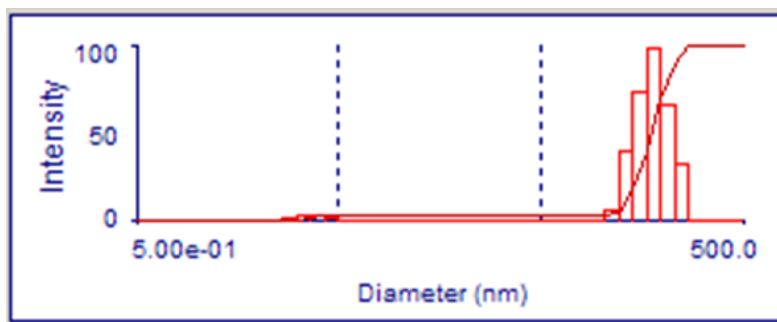


**Fig. S12.** Hydrodynamic diameter distribution of 0.5 mM Np- $\beta$ -CD aqueous solution at 298.15 K.

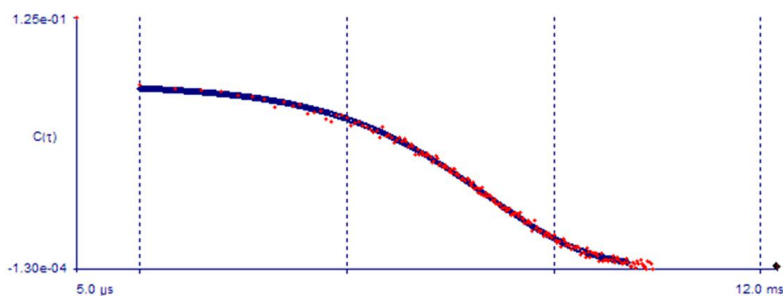


**Fig. S13.** Representative dynamic light scattering data for 0.5 mM Np- $\beta$ -CD aqueous solution.

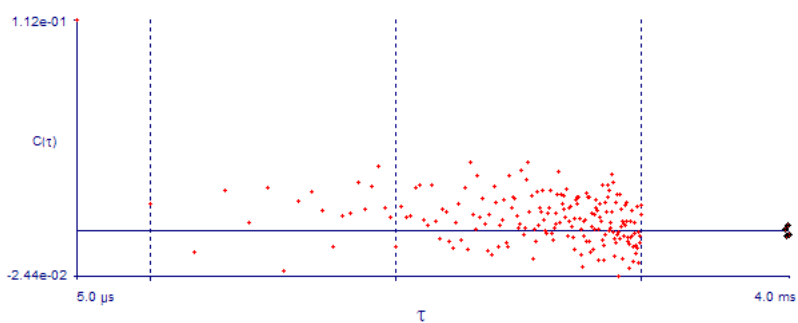


**Fig. S14.** Representative dynamic light scattering data for 0.5 mM Np- $\beta$ -CD aqueous solution with 2 equiv. compound **1**.

The aqueous solution of Np- $\beta$ -CD gave a hydrodynamic diameter of ca. 166 nm (Fig. S11), which might be attributed to the formation of Np- $\beta$ -CD self-assembly

through the penetration of naphthol group into the cavity of adjacent  $\beta$ -CD unit.<sup>2</sup> After adding 2 equiv. of **1**, no DLS signal could be observed (Fig. S13) owing to the displacement of naphthol group by the adamantyl moiety of **1** in the  $\beta$ -CD cavity, which led to the deconstruction of self-assembly.

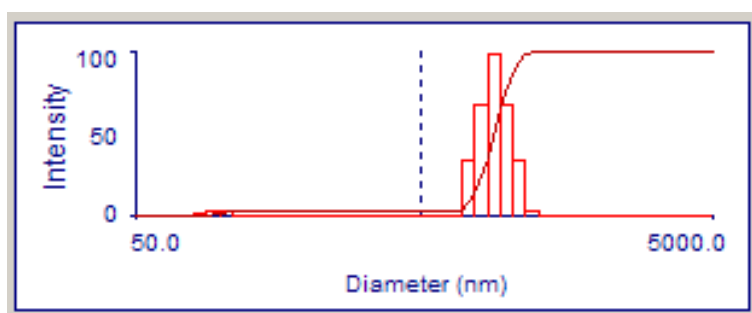


**Fig. S15.** Hydrodynamic diameter distribution of 0.5 mM Np- $\beta$ -CD/**1**/CB[8] aqueous solution at 298.15 K. The Poly value is 0.142.

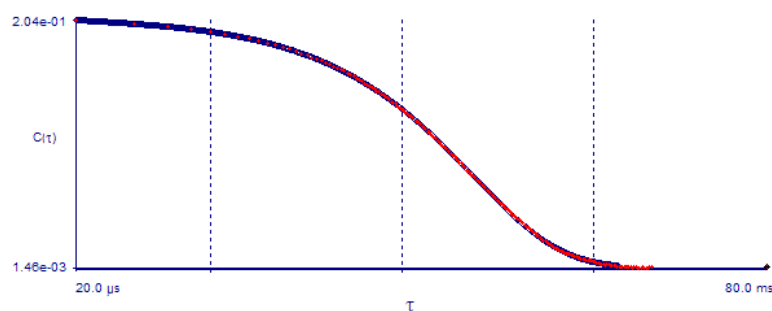


**Fig. S16.** Representative dynamic light scattering data for 0.5 mM Np- $\beta$ -CD/**1** with 1 equiv. CB[8] aqueous solution at 298.15 K.

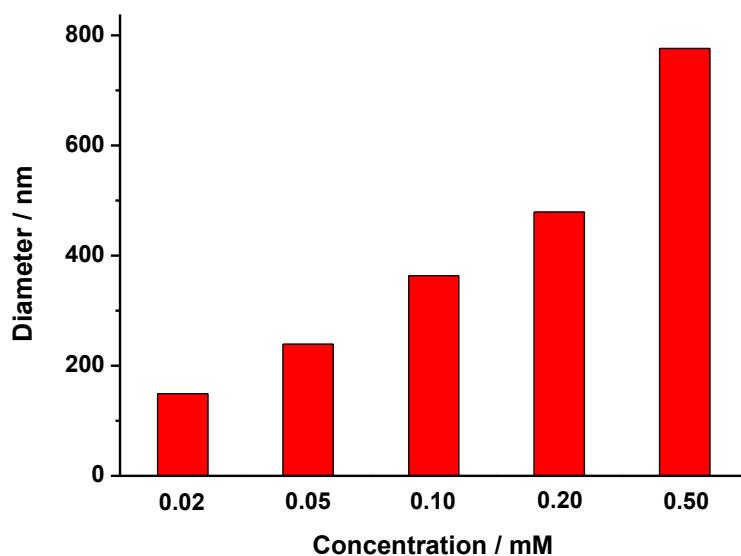


**Fig. S17.** Dependence of the hydrodynamic diameter of Np-β-CD/1/CB[8] on the supramolecular polymer concentration at 298.15 K.

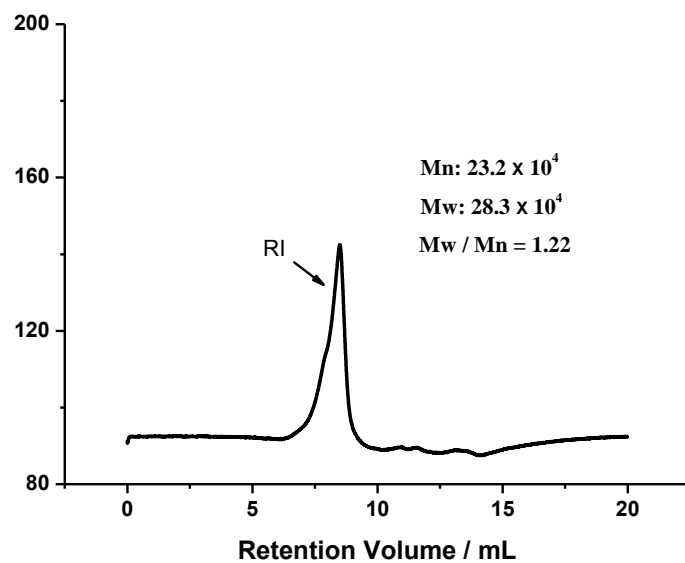


**Fig. S18.** GPC trace of 0.5 mM aqueous solution of ternary supramolecular polymer of Np-β-CD/1/CB[8] at 30 °C. The PDI value ( $M_w/M_n$ ) is 1.22.

We studied the binding behavior of **1**/CB[8] and Np- $\beta$ -CD/**1**@CB[8] by ITC. The calorimetric titration curve showed the significant heat changes of **1**/CB[8] and Np- $\beta$ -CD/**1**@CB[8] systems, clearly indicated the **1**-to-CB[8] and Np- $\beta$ -CD-to-**1**@CB[8] bindings. However, the binding constants cannot be calculated by using any of “one set of binding sites” “sequential binding sites” or “two sets of binding sites” model provided by the ITC instrument. Thus, we deduce that the **1**-to-CB[8] or Np- $\beta$ -CD-to-**1**@CB[8] binding should be a rather complicated process.

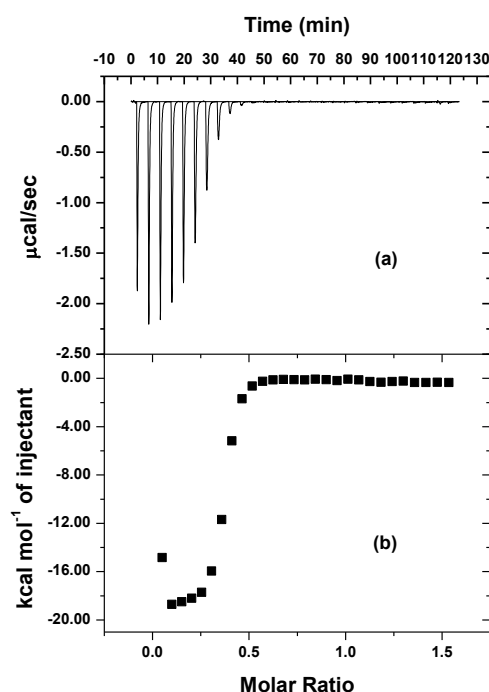


**Fig. S19** Microcalorimetric titration of **1** with CB[8] in aqueous solution at 298.15 K. (a) Raw ITC data for sequential 28 injections (10  $\mu$ L per injection) of compound **1** solution (0.35 mM) injecting into CB[8] solution (0.05 mM). (b) Apparent reaction heat obtained from the integration of calorimetric traces.

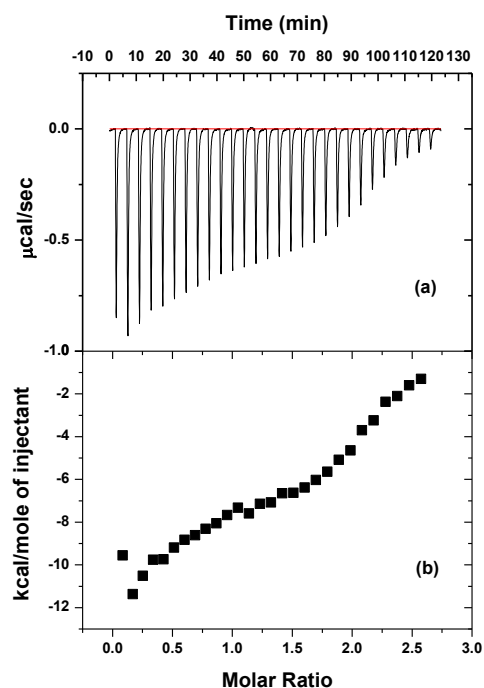


**Fig. S20** Microcalorimetric titration of Np- $\beta$ -CD with **1**@CB[8] in aqueous solution at 298.15 K. (a) Raw ITC data for sequential 28 injections (10  $\mu\text{L}$  per injection) of Np- $\beta$ -CD solution (0.29 mM) injecting into **1**@CB[8] solution (0.025 mM). (b) Apparent reaction heat obtained from the integration of calorimetric traces.

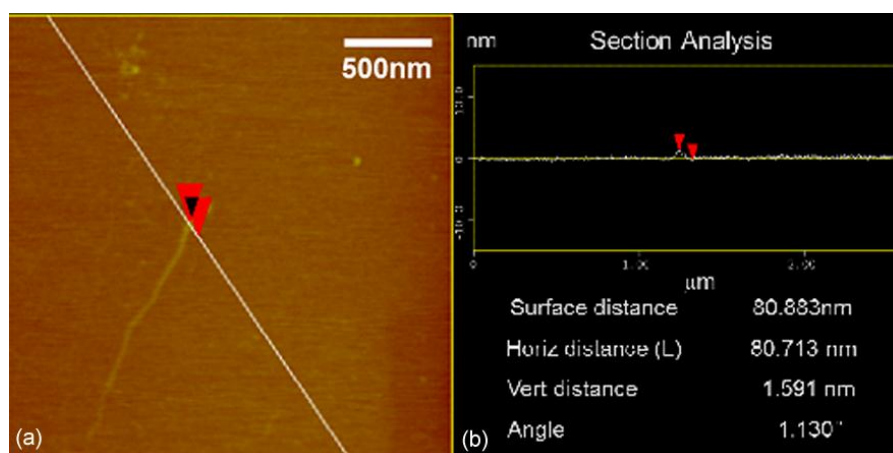


**Fig. S21.** (a) AFM image of the linear supramolecular polymer **3**. (b) Parameters of AFM image in (a).

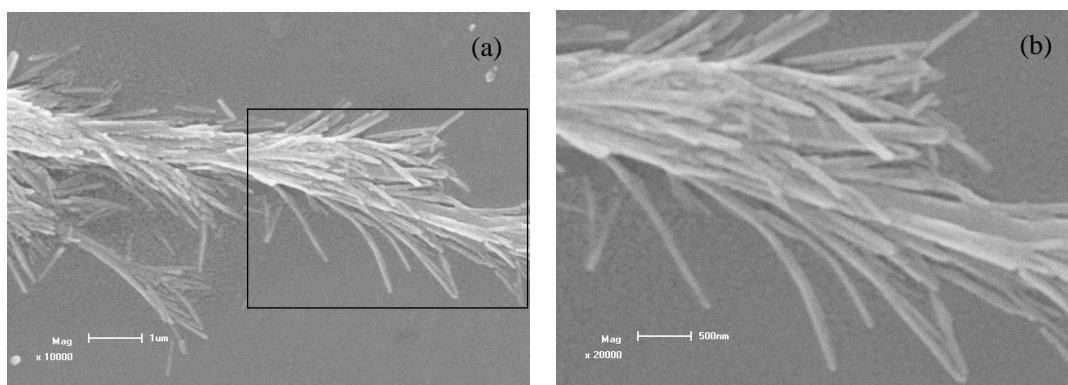


**Fig. S22.** (a) SEM image of the linear supramolecular ternary polymer **3**. (b) Magnified image of SEM in (a).

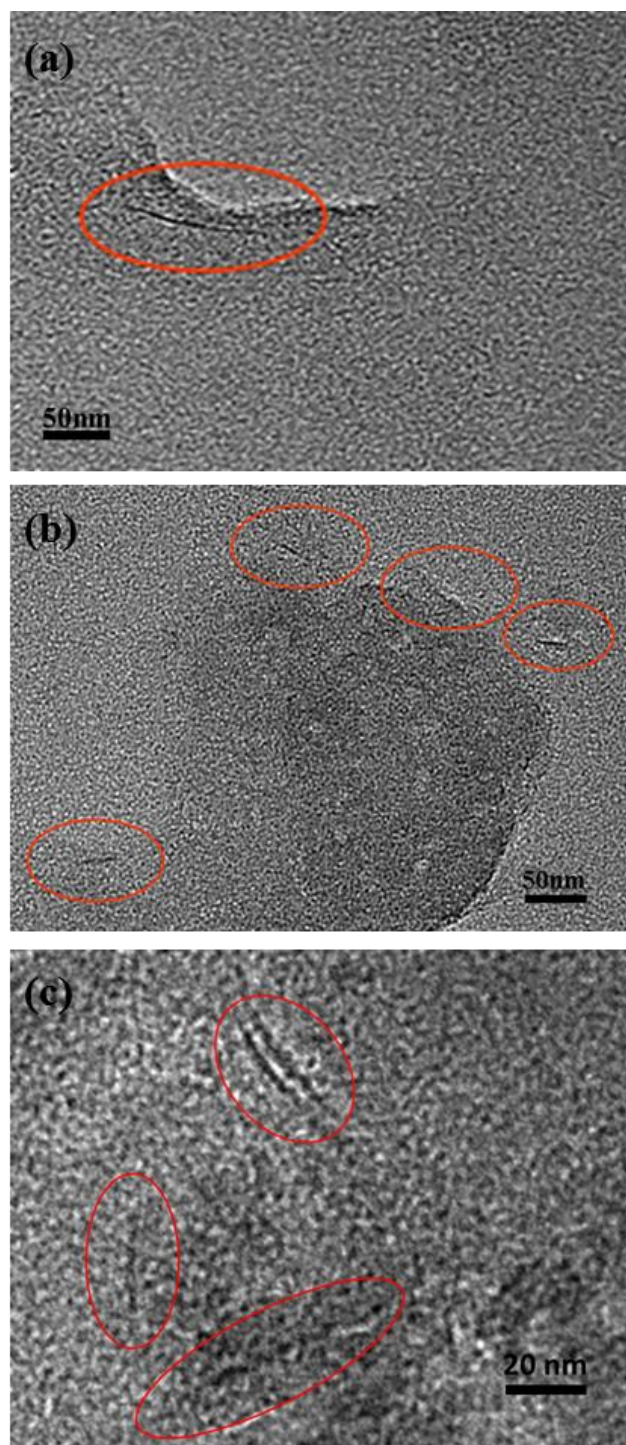


**Fig. S23** TEM images of the linear supramolecular ternary polymer **3**.

[1] Y.-M. Zhang, Y. Chen, Z.-Q. Li, N. Li, Y. Liu, *Bioorg. Med. Chem.*, 2010, **18**, 1415.

[2] Y. Liu, Z.-X. Yang, Y. Chen, *J. Org. Chem.*, 2008, **73**, 5298.